

Visible photoluminescence from *N*-dot ensembles and the linewidth of ultrasmall $\text{Al}_y\text{In}_{1-y}\text{As}/\text{Al}_x\text{Ga}_{1-x}\text{As}$ quantum dots

S. Fafard and R. Leon

Center for Quantized Electronic Structures (QUEST), University of California, Santa Barbara, California 93106

D. Leonard

Center for Quantized Electronic Structures (QUEST) and Materials Department, University of California, Santa Barbara, California 93106

J. L. Merz and P. M. Petroff

Center for Quantized Electronic Structures (QUEST) and Materials Department and Electrical and Computer Engineering Department, University of California, Santa Barbara, California 93106

(Received 27 June 1994)

Ensembles containing a few hundred quantum dots, ~ 17 nm in diameter, were prepared by etching μm -size mesas in $\text{Al}_y\text{In}_{1-y}\text{As}/\text{Al}_x\text{Ga}_{1-x}\text{As}$ quantum-dot samples grown using the spontaneous island formation during molecular-beam epitaxy. The visible photoluminescence spectra display the reproducible statistical fluctuations of the ground states, which are emitting individual lines a fraction of a meV in width.

Recent experiments performed on semiconductor quantum-dot (QD) structures obtained with the spontaneous island formation have demonstrated strong zero-dimensional (0D) confinement of the carriers in high-quality, defect-free material.¹⁻⁵ Such quantum dots were formed directly by molecular-beam epitaxy (MBE) of highly strained $\text{In}_x\text{Ga}_{1-x}\text{As}/\text{GaAs}$, giving QD's ~ 20 nm in diameter with emission in the near-infrared range at ~ 1.27 eV. That coherent islanding process can produce QD's with a size distribution smaller than $\pm 10\%$ and mean values for the diameter reaching 13 nm, as found by transmission-electron microscopy (TEM) and atomic-force microscopy.^{6,7} Using the strain-induced coherent-islanding effect with III-V materials having larger band gaps can produce similar narrow size distribution of ultrasmall QD's with emission at shorter wavelengths. In this paper, we report the achievement of quantum-dot emission in the visible range at ~ 1.88 eV (red) from $\text{Al}_y\text{In}_{1-y}\text{As}/\text{Al}_x\text{Ga}_{1-x}\text{As}$ quantum dots, ~ 17 nm in diameter, directly grown by MBE. In addition, ensembles with a relatively small number of nm-size dots can be created by delineating μm -size mesas in the samples, revealing the sharpness of the lines emitted by the individual dot. Here we focus our attention on the results of such experiments performed on ensembles containing from a few hundred to a few thousand dots. Analyzing the statistical fluctuations of the photoluminescence (PL) emitted by these *N*-dot ensembles gives important information about the optical properties of individual dots,⁸ such as the linewidth, which is found to be ~ 0.4 meV.

The dot layer is pseudomorphically grown by MBE on a (100) GaAs substrate, and the QD's are formed by the coherent relaxation into islands of a few monolayers of $\text{Al}_{0.45}\text{In}_{0.55}\text{As}$ between $\text{Al}_{0.35}\text{Ga}_{0.65}\text{As}$ buffer and cap layers. From TEM plan-view and cross-sectional measurements, the QD diameter, thickness, and density were measured. A narrow normal distribution of 17 ± 2 nm was found for the di-

ameter, and a dot density of $\sim 200 \mu\text{m}^{-2}$ and a thickness to a diameter ratio of ~ 0.18 were found. A detailed account of the growth and structural aspects, and of the general PL properties of these QD's and other samples with different $\text{Al}_y\text{In}_{1-y}\text{As}/\text{Al}_x\text{Ga}_{1-x}\text{As}$ compositions will be published separately.⁹

Figure 1(a) shows the QD PL emission measured at low

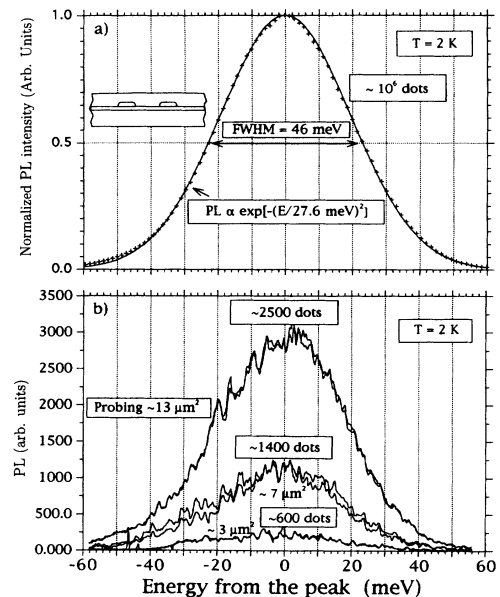


FIG. 1. (a) Typical low-temperature PL spectra obtained with a QD sample, probing a large ensemble ($\sim 10^6$) of 17-nm-diam dots under the excitation spot, and Gaussian distribution fit. (b) PL of *N*-dot ensembles delineated with μm -size mesas, displaying statistical fluctuations. Two scans are shown for each mesa to evaluate the reproducibility of the sharp features. The peak position for the $\text{Al}_y\text{In}_{1-y}\text{As}/\text{Al}_x\text{Ga}_{1-x}\text{As}$ QD ensembles is $\lambda = 660$ nm (red).

temperature (2 K) using “nonresonant” above-barrier excitation, here a few mW at $\lambda_{\text{ex}}=514.5$ or 488 nm, focused in a spot $\sim 80 \pm 20 \mu\text{m}$ in diameter, and therefore probing $\sim 10^6$ dots. The PL was dispersed with a 0.85-m double spectrometer, and detected with a cold photomultiplier. The spectrum is displayed in meV away from the peak of the emission which was in the red range at 660 nm (1.879 eV). The peak is fitted with a Gaussian distribution line shape with an inhomogeneous (extrinsic) broadening factor Γ_e of 27.6 meV, giving a full width at half maximum of 46 meV. Such smooth (structureless) spectra are typical of the case where nonresonant excitation is used, and a large number of QD’s are probed.³ It reflects the statistical distribution of the ground-state energy levels of the individual dots that arises from the slightly different 0D confining potentials. The QD’s have a deep confining potential (for example, the large difference between the energy gap of the barrier and that of the dot materials gives an electron confining potential of ~ 0.35 eV). This, combined with a relatively small height-to-diameter ratio of the dots (dot thickness ≤ 3 nm) implies that the distribution should arise mainly from the additional atoms in the growth direction (i.e., variation in the “mean” thickness of the dots). Also, other parameters, such as small variations in the diameter, in the alloy composition, or in partial (defect-free) strain relaxation, can also contribute to the observed inhomogeneous broadening.

The ultimate confirmation of the QD nature of the emission is obtained by measuring the PL emitted by a smaller number of QD’s contained in mesas of different sizes patterned after these samples; see Fig. 1(b), which shows the 2-K results. Arrays of μm -size mesas separated from each other by $140 \mu\text{m}$ were obtained by standard photolithography and wet chemical etching, removing completely the QD and $\text{Al}_x\text{Ga}_{1-x}\text{As}$ cap and buffer layers with $\text{H}_2\text{O}_2:\text{H}_2\text{SO}_4:\text{H}_2\text{O}$ (1:1:20) in the unprotected regions. The small mesas are therefore used to delineate the number of QD’s probed in a controlled fashion. Figure 1(b) shows results obtained with 3, 7, and $13 \mu\text{m}^2$ mesas corresponding, respectively, to $N \sim 600$, 1400, and 2500 dots probed. For the small mesas containing only a few hundred dots, the PL spectra display distinct, extremely narrow (small fraction of a meV) lines. Note that all the figures presenting experimental results in this paper display two consecutive scans of the same mesa in order to give a good representation of the reproducibility of all the sharp spectral features. As the number of dots probed increases, the spectra become smoother, as expected, by considering the statistics of large numbers of convoluted lines. The larger ensembles with 2500 dots still show very clear statistical fluctuations, implying that the homogeneous (or intrinsic) broadening Γ_i for the radiative recombination process in an individual 0D structure is much smaller than the Γ_e found above. Small statistical fluctuations were still observable with ensembles as large as $N \sim 19\,000$ (not shown), but then the spectra essentially display the structureless distribution of the emitting energy of the ensemble of dots, as is the case if no mesas are used to delineate the number of dots probed under the excitation spot as in Fig. 1(a).

For two different small QD subsets, the statistical fluctuations will give two different (but reproducible) spectra lying within the Γ_e boundaries. This is readily verified experimen-

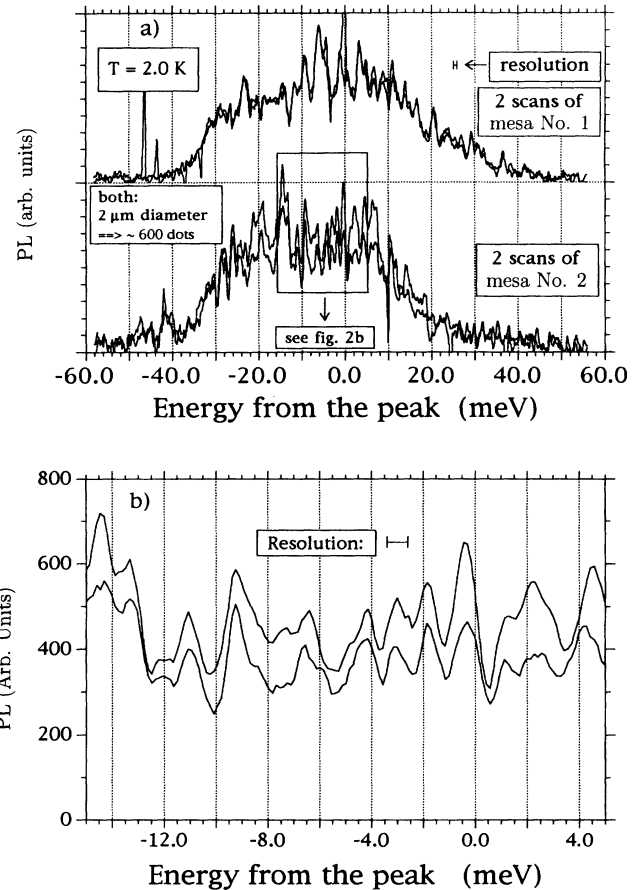


FIG. 2. (a) PL spectra obtained with a spectral resolution of 0.8 meV on two different mesas and (b) expanded scales.

tally, since the lithographic mask which is used in our experiment provides rows of mesas with the same dimensions (~ 7 mesas per mm). Such PL results obtained on two different mesas both containing ~ 600 dots are shown in Fig. 2(a). Good reproducibility of the sharp features was always observed for a given ensemble but, as expected, different sets of lines are observed for different ensembles. Many of the sharp features observed are not spectrally resolved if the spectrometer resolution is set to 0.8 meV, as can be better seen in Fig. 2(b), which expands part of the spectra of Fig. 2(a).

In order to obtain more qualitative and quantitative information, the spectra and the resulting fluctuations can be simulated for different ensembles. The simulations assume a number N of independent (uncoupled) dots emitting lines of equal amplitude, and with the same homogeneous broadening Γ_i , randomly distributed in energy within a broader ($\Gamma_e > \Gamma_i$) Gaussian distribution. The inhomogeneous broadening is set to $\Gamma_e = 27.6$ meV to match the experimental value, and Γ_i and N are varied. Also, because the experimental spectra agree well with a single symmetric distribution for the excitation used, we assume there is no emission originating from excited-state transitions. In the limit of large N , the smooth structureless Gaussian distribution characterized by Γ_e will be recovered. The actual value of N at which the spectra are essentially smooth depends only on Γ_i , since

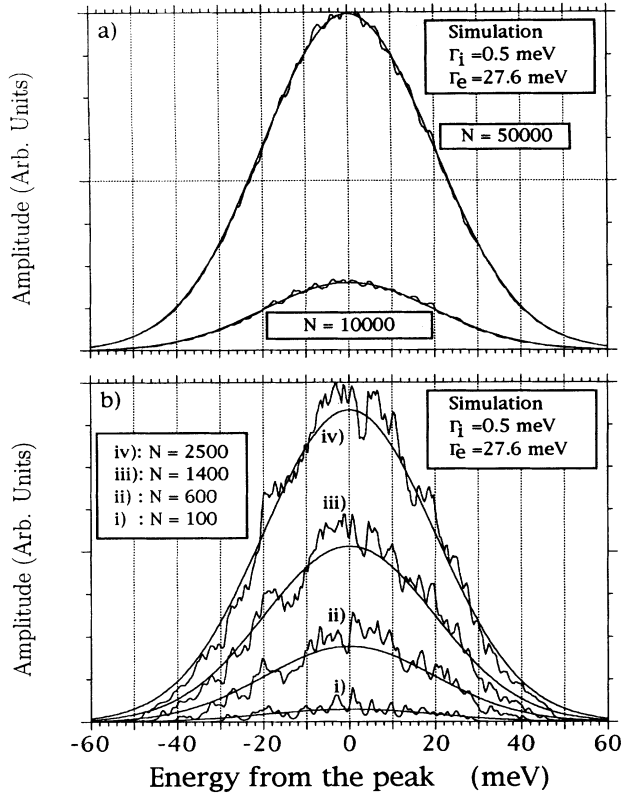


FIG. 3. Simulations displaying the statistical fluctuations of N narrow lines with a homogeneous broadening Γ_i , randomly distributed with a Gaussian inhomogeneous broadening Γ_e .

Γ_e is fixed. For example, Fig. 3(a) shows simulated spectra obtained with $\Gamma_i = 0.5$ meV, for $N = 10\,000$ and $N = 50\,000$. In this case, fairly smooth curves are obtained, as seen by comparing with the smooth bell curve, which is the Gaussian distribution having the same area (i.e., $G(E) = A_e \exp[-(E - E_0)^2 / \Gamma_e^2]$, where $A_e = Na_i / \pi^{1/2} \Gamma_e \approx N \Gamma_i / \Gamma_e$ and a_i is the area of the normalized homogeneous line¹⁰). It is also clear from such simulations that for reasonable values of Γ_i , “perfectly” smooth curves are obtained for $N \sim 10^6$, such as in the case of PL experiments with no mesas. For small ensembles, however, $\Gamma_i = 0.5$ was found to give a good reproduction of the amplitude of the statistical fluctuations observed experimentally. This can be seen by qualitatively comparing the simulation of Fig. 3(b) with the spectrum obtained with the QD ensembles with the corresponding number of dots in Fig. 1(b). From the simulations, it is also clear that it becomes difficult to observe isolated QD contribution as N increases above a few times Γ_e / Γ_i . The spikes that rise above the mean distribution are often a contribution of several nearby lines, but the simulations show that the sharpest features of the small ensembles can be used to get an upper bound estimate on the value of Γ_i .

In order to get more quantitative information from the simulation, the normalized density of statistical fluctuations¹¹ can be plotted as a function of N for different values of Γ_i . For example, Fig. 4 shows the results from simulations obtained with $\Gamma_i = 1.00, 0.50,$ and 0.25 meV. The normalized density of statistical fluctuations decreases with increasing N

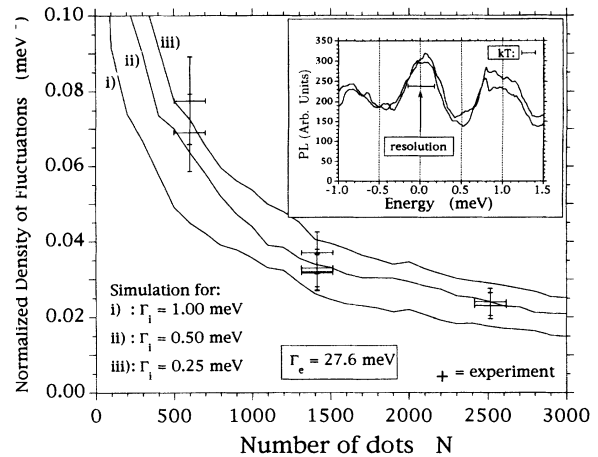


FIG. 4. Normalized density of fluctuations (i.e., the root-mean-square deviation divided by the curve area) obtained from simulations with various Γ_i (solid lines), and experimental values from the spectra of Fig. 1(b) (crosses). The inset shows a 2.0-K, high-resolution (0.3 meV) spectrum with a sharp (0.4 meV) feature.

roughly as $N^{-1/2}$, and increases for smaller Γ_i . By comparing the values found experimentally for the normalized density of fluctuations with N -dot ensembles it is possible to obtain an estimate of Γ_i . For example, the crosses in Fig. 4 show results for $N \sim 600, 1400,$ and 2500 , obtained from the spectra of Fig. 1(b). The data fall close to and above the $\Gamma_i = 0.5$ meV line. The accuracy of the results depends on the exact number of dots contained in the mesa, and the ability to fit the experimental spectra in order to evaluate the normalized density of the statistical fluctuations. The number of dots in a given mesa can change if there are some local variations in the density of QD's and from small variations in the size of the etched mesas, but are generally accurate to $\pm \sim 100$ dots. The fit of the spectra can be affected by experimental noise or shape asymmetry, but the reproducibility of spectra and the Gaussian fit of Fig. 1(a) are very good. There is, however, a trade-off between increasing the resolution and avoiding external noise. In the present case, the density of fluctuations is probably underestimated because not all the features were spectrally resolved. For example, the inset of Fig. 4 also shows a high-resolution spectrum with sharp features from a 600-dot mesa. The ~ 0.4 -meV-wide feature center at 0 meV appears to be resolved with a spectrometer resolution of 0.32 meV but, as shown with the above simulation, that peak could very well represent the contributions of a number of dots with very similar energies. This would set the value of $2\Gamma_i \sim 0.4$ meV, which is in agreement with the normalized density of fluctuations measured with the 600-dot mesas. The fact that the larger ensembles tend to indicate smaller density of fluctuations and, therefore, larger Γ_i might suggest that some islands have a slightly larger Γ_i , or that some collective behavior might result in smoothing effects.

In conclusion, N -dot ensembles with a relatively small number of nm-size dots can be created by delineating μm -size mesas photolithographically in QD samples prepared by the spontaneous island formation. The sharpness of

the lines emitted by the individual dots reveals itself through statistical fluctuations and sharp features in the photoluminescence spectra. The full width at half maximum of the radiative recombination of photocarriers in single 17-nm-diameter dots with strong confinement in high-quality $\text{Al}_{1-y}\text{In}_y\text{As}/\text{Al}_x\text{Ga}_{1-x}\text{As}$ material, directly grown by molecular-beam epitaxy, was estimated to be 0.4 meV or smaller. These quantum dots yield bright luminescence in the visible range, for example, the red luminescence from 600-dot ensembles are visible with the naked eye. Other experiments, such as photoluminescence excitation, photoluminescence excited resonantly, or time-resolved pho-

toluminescence, can be performed on such *N*-dot ensembles to reveal more details about the excited energy levels and the carrier dynamics. Also, recent cathodoluminescence experiments^{12,13} have provided spatial resolution of the emission.

This research was supported by NSF Science and Technology Center QUEST (DMR Grant No. 91-20007), and by AFOSR Grant No. F49620-92-J-0124. We would like to thank E. Caine and E. Hu for their help with the photolithography of the mesas. One of us (S.F.) would also like to acknowledge NSERC of Canada for its support.

¹D. Leonard, M. Krishnamurthy, C. M. Reaves, S. P. Denbaars, and P. M. Petroff, *Appl. Phys. Lett.* **63**, 3203 (1993).

²D. Leonard, M. Krishnamurthy, S. Fafard, J. L. Merz, and P. M. Petroff, *J. Vac. Sci. Technol. B* **12**, 1063 (1994).

³S. Fafard, D. Leonard, J. L. Merz, and P. M. Petroff, *Appl. Phys. Lett.* (to be published).

⁴G. Wang, S. Fafard, D. Leonard, J. E. Bowers, J. L. Merz, and P. M. Petroff, *Appl. Phys. Lett.* **64**, 2815 (1994).

⁵Although not presented in a QD context, older works also suggest such 0D confinement in similar structures, e.g., L. Goldstein, F. Glas, J. Y. Marzin, M. N. Charasse, and G. Le Roux, *Appl. Phys. Lett.* **47**, 1099 (1985).

⁶D. Leonard, K. Pond, and P. M. Petroff, *Phys. Rev. B* (to be published).

⁷J. M. Moison, F. Houzay, F. Barthe, L. Leprince, E. André, and O.

Vatel, *Appl. Phys. Lett.* **64**, 196 (1994).

⁸Single dots with relatively shallow parabolic confinement have been studied by K. Brunner, U. Bockelmann, G. Abstreiter, M. Walther, G. Böhm, G. Tränkle, and G. Weimann, *Phys. Rev. B* **49**, 3216 (1994).

⁹R. Leon, S. Fafard, D. Leonard, P. M. Petroff, and J. L. Merz (unpublished).

¹⁰The normalized homogeneous line area $a_i = \pi\Gamma_i$ for a Lorentzian line shape, or $a_i = \pi^{1/2}\Gamma_i$ for a Gaussian line shape.

¹¹The normalized density of fluctuation is defined using the root-mean-square deviation and dividing by the area: $A_e^{-1}\{\sum_i [PL(E_i) - G(E_i)]^2\}^{1/2}$.

¹²R. Leon, S. Fafard, P. M. Petroff, and J. L. Merz (unpublished).

¹³M. Grundmann *et al.* (unpublished).